20 July 2001

ELSEVIER

Chemical Physics Letters 342 (2001) 652–658

CHEMICAL PHYSICS LETTERS

www.elsevier.com/locate/cplett

Charge redistribution and electronic polarization in organic molecular crystals

Z.G. Soos *, E.V. Tsiper, R.A. Pascal Jr.

Department of Chemistry, Princeton University, Princeton, NJ 08544, USA

Received 9 March 2001; in final form 22 May 2001

Abstract

The electronic polarization of organic molecular crystals is obtained using the atom–atom polarizability tensor and charge redistribution in addition to previous theory based on induced dipoles. The dielectric tensors of anthracene and perylenetetracarboxylic acid dianhydride (PTCDA) crystals are successfully related to molecular polarizabilities.

1. Introduction

Silinsh and Capek [1] discuss in detail the polarization energy of ions in organic molecular crystals, with particular attention to acenes. These crystals are insulators whose structure and spectra closely resemble the gas phase, and exciton theory assumes an oriented gas of molecules that respond to applied or internal electric fields. The energies of charges and charge-transfer states are important for recent electronic applications of organic crystals or thin films and charges lead to strong, long-range interactions for typical dielectric constants of $\varepsilon \sim 3$. Theoretical approaches to polarization rely on induced dipoles, as done by Mott and Littleton [2] for atomic lattices. Munn and coworkers [3–5] have found self-consistent solutions for ions and ion pairs, and for crystals in a uniform field **E**. In their analysis, the *crystal* structure and *molecular* polarizability α are known by hypothesis and intermolecular overlap is neglected. Submolecules [6,3] with fractional α at rings are used for tetracene or pentacene, whose size exceeds van der Waals contacts. Perylenetetracarboxylic acid dianhydride (PTCDA, Fig. 1) requires 11 submolecules at the centers of rings and C=O bonds [7]. Recent applications include polar molecules and acenes with dipoles at carbon atoms [8]. Although submolecules are physically motivated for conjugated systems, their ad hoc nature is well recognized [1,7,8].

We introduce in this Letter another approach to electronic polarization and apply it to the dielectric tensors of anthracene and PTCDA crystals. We retain the crystal structure, the molecular polarizability, and continue to neglect intermolecular overlap. Instead of submolecules, however, we compute the atom–atom polarizability tensor Π_{kp} and find explicitly how charge redistributes in the crystal's field. We distinguish between molecular and atomic contributions to α. Conjugated molecules are 'atomic' for **E** normal to the plane; the field distorts orbitals and induces dipoles. In-plane fields yield the large linear and nonlinear responses that are universally understood as delocalization.

* Corresponding author. Fax: +1-609-258-6746.
E-mail address: soos@princeton.edu (Z.G. Soos).

0009-2614/01/$ - see front matter
PII: S0009-2614(01)00661-3

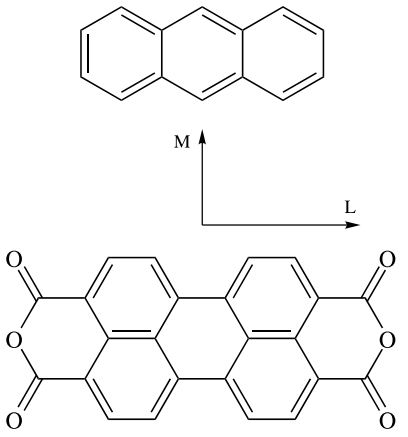

Fig. 1. Schematic representation of anthracene and PTCDA molecules, with long (L) and medium (M) principal axes of the polarizability tensor fixed by D_{2h} symmetry.

Charge redistribution is 'molecular' and involves coefficients of atomic orbitals that in Hückel theory are not polarizable at all.

For simplicity, we consider centrosymmetric molecules with atoms at $\mathbf{a}_k$ from the center of the molecule. The charge density $\rho(\mathbf{r}) = |\Psi(\mathbf{r})|^2$ is the same at $-\mathbf{r}$. The induced dipole is

$$\boldsymbol{\mu}(\mathbf{E}) = \alpha \cdot \mathbf{E} = \int \mathbf{r}\rho(\mathbf{r}, \mathbf{E})\, \mathrm{d}v = \sum_k \{\mathbf{a}_k \rho_k(\mathbf{E}) + \boldsymbol{\mu}_k(\mathbf{E})\}. \quad (1)$$

The sum is over atoms with partial charges ρ_k and dipoles $\boldsymbol{\mu}_k$ whose precise definitions depend on how volume or overlap is partitioned. The partitioning is irrelevant in a uniform field and α describes the entire linear response. Crystal fields are not uniform over large molecules, however. The tensor Π_{kp} defined below in (3) gives the response to changes in the electrostatic potential at any pair of atoms k,p; it controls the redistribution of $\rho_k(\mathbf{E})$ in (1). The first sum in (1) is the molecular part, $\alpha_M \cdot \mathbf{E}$, which corresponds to charge flow in π-systems. We attribute the remainder, $(\alpha - \alpha_M) \cdot \mathbf{E}$, to induced dipoles whose treatment follows previous theory [3]. Then $\boldsymbol{\mu}_k = \alpha_k \cdot \mathbf{E}_k$ is the atomic contribution to (1) and we formally have submolecules, now taken as atoms, to describe the distortion of atomic orbitals under local fields. The physical difference is that $\boldsymbol{\mu}_k(\mathbf{E})$ conserves charge about each atom while $\alpha_M \cdot \mathbf{E}$ redistributes it over molecular distances.

Coulson and Longuet-Higgins [9] defined the mutual π-electronic polarizability of atoms [10]. The electrostatic potential or site energy ε_k of atom k is related to ionization potentials in semiempirical methods. A uniform field gives $\varepsilon_k = -\mathbf{a}_k \cdot \mathbf{E}$ and atom–atom polarizability Π_{kp}

$$\alpha_M = \sum_{kp} \mathbf{a}_k \Pi_{kp} \mathbf{a}_p. \quad (2)$$

It follows at once that $\mathbf{E}$ normal to a planar molecule is orthogonal to all $\mathbf{a}_k$. We include all valence electrons, not just π-electrons, to find α_M and treat Π as a susceptibility. This differs by a factor of $-1/2$ from the original tensor π [9]. The links of Π_{kp} to Hückel models and one-electron theory rationalize why charge redistribution is far easier to compute than atomic polarizabilities. Moreover, since $\boldsymbol{\mu}_k(\mathbf{E})$ is related to $\alpha - \alpha_M$, approximations in Π are partly compensated by induced dipoles when α is known accurately.

Self-consistent dipolar fields appear in the previous analysis [1,3] of induced dipoles. We extend the oriented gas model to include self-consistent atomic charges $\rho_k(\mathbf{E})$ and Coulomb fields. We present the general solution for any distribution of fixed charges and then use translational symmetry to compute the electronic dielectric tensor, or index of refraction, of anthracene and PTCDA crystals.

2. Charge redistribution

We consider a molecule or ion s with atoms at $\mathbf{a}_k$, electronic energy W_s, and site perturbations $\varepsilon_k n_k$, with $\varepsilon_k = 0$ in the unperturbed system. The number operators n_k refer to valence electrons. As in π-electron theory [10], Taylor expansion of $W_s(\varepsilon_k)$ yields atomic charges $\rho_k^{(0)}$ in first order and Π_{kp} in second order, with

$$\Pi_{kp}^{(s)} = -\left(\frac{\partial^2 W_s}{\partial \varepsilon_k \partial \varepsilon_p}\right)_0 = 2 \sum_R{}' \frac{\langle G|n_k|R\rangle\langle R|n_p|G\rangle}{E_R - E_G}. \quad (3)$$

The order of the symmetric matrix Π is the number of atoms. The formal sum is over exact excited states with energy E_R, excluding $R = G$, and is related to the second-order correction $W_s^{(2)}$ to site perturbations. The susceptibility is actually computed as second derivatives of W_s with respect to ε_k. We have different Π_{kq} for the ground states of molecules, cations and anions. INDO/S [11] is well suited for repetitive calculations: it is fast, ε_k can readily be varied, and spectroscopic parametrization yields satisfactory α_M. We expand [12] the wavefunction in terms of orthogonal atomic orbitals to obtain Löwdin charges $\rho_k^{(0)}$. The change in atomic charge is

$$\rho_k^{(s)} = \left(\frac{\partial W_s}{\partial \varepsilon_k}\right)_{\varepsilon} = \rho_k^{(0)} - \sum_p \Pi_{kp}^{(s)} \varepsilon_p. \tag{4}$$

The partial derivative of $W_s(\varepsilon_k)$ automatically takes into account the molecule's internal energy. Net charge $\sum \rho_k^{(s)}$ is conserved since, as seen in (3), we have $\langle G|\sum n_k|R\rangle = 0$ by orthogonality for systems with a fixed number of electrons. Charge conservation on individual molecules is the key simplification that follows from neglecting intermolecular overlap and is central to our analysis. For the special case of a uniform field, we insert $\varepsilon_p = -\mathbf{a}_p \cdot \mathbf{E}$ in (4) and substitute into (1) to obtain α_M in (2).

In the crystal, we associate volume V_M with each molecule, take the origin at the molecular center, and find the electrostatic potential $\varphi(\mathbf{r})$ in V_M. The atoms k of the reference molecule have $\mathbf{r} = \mathbf{r}_k\ (= \mathbf{a}_k)$ and $\varphi(\mathbf{r}_k)$ can be viewed as a site energy ε_k. The crystal potential in a uniform field is

$$\varphi(\mathbf{r},\mathbf{E}) = -\mathbf{r}\cdot\mathbf{E} + {\sum_{nm}}' \Big\{ \rho_n^m(\mathbf{E})/|\mathbf{r}-\mathbf{r}_n^m| + \boldsymbol{\mu}_n^m(\mathbf{E})\cdot(\mathbf{r}-\mathbf{r}_n^m)/|\mathbf{r}-\mathbf{r}_n^m|^3 \Big\}. \tag{5}$$

The sum is over atoms n at $\mathbf{r}_n^m$ in all other molecules m, and $\mathbf{r}$ is in V_M. Atomic charges and dipoles generate Coulomb and dipolar potentials, respectively. The corresponding fields, $-\nabla\varphi(\mathbf{r},\mathbf{E})$, induce dipoles. The general problem gives four simultaneous linear equations at each atom [12],

$$\begin{aligned} \rho_k^{(s)} - \rho_k^{(0)} &= -\sum_p \Pi_{kp}^{(s)} \varphi(\mathbf{r}_p,\mathbf{E}), \\ \boldsymbol{\mu}_k^{(s)} - \boldsymbol{\mu}_k^{(0)} &= -\alpha_k^{(s)} \cdot \nabla\varphi(\mathbf{r}_k,\mathbf{E}). \end{aligned} \tag{6}$$

Since Π_{kp}, α_k and all distances are specified, the potentials and fields due to $\mathbf{E}$ or $\rho_k^{(0)}$ alter the charges and induce dipoles that, in turn, modify $\varphi(\mathbf{r},\mathbf{E})$ and its gradient. The dipole moment of polar molecules is given by $\mathbf{E} = 0$ in (1); it is the sum of molecular contributions, $\sum_k \mathbf{a}_k \rho_k^{(0)}$, and atomic terms $\boldsymbol{\mu}_k^{(0)}$ that both vanish for nonpolar molecules. An iterative solution [12] of (6) is based on alternately updating atomic charges and dipoles, and then potentials and fields, for a specified distribution of molecules and molecular ions. A modern computer workstation can conveniently handle 10^4–10^5 atoms.

3. Electronic dielectric constant

For the electronic dielectric constant, we take all molecules in the ground state and drop the index 's'. Translational symmetry ensures equal $\rho_k\mathbf{E}$ and $\boldsymbol{\mu}_k(\mathbf{E})$ in unit cells of Z molecules with Q atoms each. We have $4ZQ$ simultaneous equations in (6). The lattice gives Madelung or dipolar sums that are found by Ewald's method [13,14]. The geometrical sums are, for each atom in the unit cell,

$$M_n(\mathbf{r}) = {\sum_m}' \Big\{ |\mathbf{r}-\mathbf{r}_n^m|^{-1} - |\mathbf{r}-\mathbf{r}^m|^{-1} \Big\}. \tag{7}$$

All denominators are finite because the prime excludes atoms in the reference molecule. The second term is an equal and opposite charge at the center of molecule m to ensure convergence; these contributions cancel exactly for neutral molecules with $\sum \rho_k(\mathbf{E}) = 0$. For one molecule per unit cell, the double sum in (5) reduces to

$$\varphi(\mathbf{r},\mathbf{E}) = -\mathbf{r}\cdot\mathbf{E} + \sum_n \{\rho_n(\mathbf{E}) M_n(\mathbf{r}) - \boldsymbol{\mu}_n(\mathbf{E})\cdot\nabla M_n(\mathbf{r})\} \tag{8}$$

with $\mathbf{r}$ in V_M. The general case has additional interactions between atoms of different molecules in the cell [12]. The potentials due to atomic charges and induced dipoles lead to fields $-\nabla\varphi(\mathbf{r},\mathbf{E})$ that act on induced dipoles. The dipole-field tensor [3] $T_n^{\alpha\beta}(\mathbf{r})$ is $\partial^2 M_n(\mathbf{r})/\partial r_\alpha \partial r_\beta$ and couples dipoles on different molecules.

Anthracene ($C_{14}H_{10}$, $Z = 2$) crystals [15] lead to 192 simultaneous equations (6) when $\varphi(\mathbf{r},\mathbf{E})$ is

given by (8). The number is 304 for PTCDA ($C_{24}H_8O_6$, $Z = 2$) crystals [16]. Both crystals are monoclinic, with unique b axis. We solve for $\rho_k(\mathbf{E})$ and $\boldsymbol{\mu}_k(\mathbf{E}) = -\alpha_k \cdot \nabla\varphi(\mathbf{r}, \mathbf{E})$ for $\mathbf{E}$ along the orthogonal directions $\mathbf{b}$, $\mathbf{c}$ and $\mathbf{a}^*$. The unit-cell polarization for each orientation is

$$\mathbf{P}(\mathbf{E}) = \sum_k \{\rho_k(E)\mathbf{a}_k - \alpha_k \cdot \nabla\varphi(\mathbf{r}_k, \mathbf{E})\}/V_c \equiv \zeta \cdot \mathbf{E} \tag{9}$$

The sum is over the atoms in the unit-cell volume, $V_c = 2V_M$. The matrix ζ defined by (9) has principal axes $2 = b$, 1, and 3, and principal values ζ_{11}, ζ_{bb}, ζ_{33}. The uniform applied field $\mathbf{E}$ appears in (9), while the desired susceptibility χ_e in $\mathbf{P} = \chi_e\mathbf{F}$ involves the total field, $\mathbf{F} = \mathbf{E} - 4\pi\mathbf{P}/3$. The second term is the field due to the assumed spherical sample. With $\mathbf{E}$ along a principal axis, we have algebraic equations and eliminate $\mathbf{E}$ in favor of $\mathbf{F}$ to obtain the principal indices of refraction

$$n_1^2 = \varepsilon_{11} = 1 + 4\pi\zeta_{11}/(1 - 4\pi\zeta_{11}/3). \tag{10}$$

The principal axes 1 and 3 of n^2 or ε are in the ac plane, while $2 = b$. We can also obtain (10) by considering $\mathbf{E} = \mathbf{E}_0 + 4\pi\mathbf{P}/3$ in (9) to be the local field produced by a macroscopic field $\mathbf{E}_0$ and the polarization of other molecules. Along principal axes, the displacement $D = \mathbf{E}_0 + 4\pi\mathbf{P}$ and $\varepsilon = D/\mathbf{E}_0$ lead to (10). Both the directions and magnitudes are related to gas-phase (α, Π) and structural data in the limit of no intermolecular overlap.

The crystal gives all distances and INDO/S yields Π in (3) and α_M in (2). These inputs are fixed. The molecular tensor α in (1) is a completely independent quantity in the approximation of an oriented gas, and either measured or calculated α can be used; α is ultimately the reason for charge redistribution and induced dipoles in the crystal. Anthracene and PTCDA have D_{2h} symmetry with the long (L) and medium (M) principal axes in Fig. 1 fixed by symmetry. The normal (N) axis has the smallest, purely atomic α_{NN} whose accurate calculation is demanding. The B3LYP [17] functional with a 6-31G(d) basis is a widely used, normally reliable hybrid density-functional theory that gives less than half of α_{NN} for anthracene. Table 1 lists measured [18,19] principal components for anthracene, B3LYP results with the larger 6-311++G(d,p) basis, and INDO/S results for α_M in (2) that, as expected, are restricted to the plane. MP2 calculations with the same basis give slightly lower values. The TZVP-FIP values from [8] use a comparable triple-zeta basis with a different exchange potential and special field-induced polarization functions. We are studying larger bases in which PTCDA is still feasible and emphasize that α is a separate problem. Table 1 also has PTCDA principal components with the larger B3LYP basis and similar in-plane α_M results. The atomic part of (1) is the difference $\alpha - \alpha_M$ between the molecular polarizability and charge redistribution. As in previous work [3,7,8], we evaluate $\mathbf{E}_k$ at the assumed induced dipoles. We distributed $\sum_k \alpha_k = \alpha - \alpha_M$ according to the number of valence electrons at atom k. Since the atomic part is a correction to charge redistribution, the magnitude and location of induced dipoles are less important.

Each choice of α yields an electronic dielectric tensor (10) with different principal values and

Table 1
Principal components of the molecular polarizabilities of anthracene and PTCDA along the axes shown in Fig. 1; α_{eff} is obtained from the experimental dielectric tensor in Table 2

Molecule	Method	α_{NN} (Å^3)	α_{MM} (Å^3)	α_{LL} (Å^3)
Anthracene	Expt. [18,19]	15.2/15.9	25.6/24.5	35.2/35.9
	B3LYP/6-311++G(d,p)	12.03	24.27	42.56
	MP2/6-311++G(d,p)	12.12	23.43	39.38
	TZVP-FIP [8]	12.82	25.44	44.92
	INDO/S, α_M, Eq. (2)	0	24.05	41.52
	α_{eff}	14.1	24.8	42.4
PTCDA	B3LYP/6-311++G(d,p)	18.06	50.27	88.18
	INDO/S, α_M, Eq. (2)	0	50.84	84.54

Table 2
Principal componets of the dielectric tensor and indices of refraction, $\varepsilon = n^2$, of crystalline anthracene and PTCDA

Crystal	Inputs	ε_{11}	ε_{bb}	ε_{33}
Anthracene	Expt [20–23], mean	2.49(10)	3.07(10)	4.04(20)
	α/TZVP-FIP	2.35	3.09	4.31
	α/B3LYP/6-311++G(d,p)	2.23	2.91	4.03
	α/MP2/6-311++G(d,p)	2.22	2.83	3.72
	α/expt., mean	2.69	3.14	3.39
	α_M, Eq. (2)	1.36	2.39	3.90
PTCDA	Expt. [24]	1.9(1)/1.85	4.3(2)/4.07	4.6(2)/4.07
	αB3LYP/6-311++G(d,p)	1.96	3.98	4.00
	α_M, Eq. (2)	1.01	3.75	3.78

The calculated ε are based on the indicated α in Table 1; the unique axis is ε_{bb}; ε_{11}, ε_{33} are in the ac plane.

orientation in the ac plane. Table 2 presents calculated results; 'α/expt' is the mean of the measured α in Table 1. Crystal data for anthracene are based on two measurements each of the dielectric constant [20,21] and the refractive indices [22,23]. The angle $\theta = 28 \pm 2°$ between ε_{11} and **a** fixes the orientation in the ac plane. The calculated principal values in Table 2 are satisfactory with either triple-zeta basis. Charge redistribution successfully bridges molecular and crystal data without adjustable parameters in the oriented-gas model. The calculated θ is 31.6° for the expt and B3LYP polarizabilities and 31.8° for TZVP and MP2. We can also go from the oriented gas to molecules. The principal components ε_{ii} in Table 2 are reproduced exactly by the reasonable α_{eff} of Table 1, although with $\theta = 33.0°$. We see that $\sim$5% variations of α yield similar changes in ε.

The PTCDA results in Table 2 are for crystalline thin films [24]. Since the two PTCDA stacks are not quite at right angles, there is a small anisotropy in the ac plane that has not yet been identified experimentally. The dielectric tensor and indices of refraction are close to axial, with ε_{11} nearly normal to the molecular planes. The B3LYP/6-311++G(d,p) polarizabilities again account for the crystal data. The α_M results, which only include charge redistribution and neglect induced atomic dipoles, gives the in-plane response but fail completely for ε_{11}. The PTCDA lattice illustrates the distinction between charge redistribution leading to α_M and orbital distortions in $\alpha - \alpha_M$.

4. Discussion

Charge redistribution and its self-consistent calculation in organic molecular crystals are new results. (6) for ρ_k and $\boldsymbol{\mu}_k$ reduce to induced dipoles when neutral molecules are shrunk to a point ($\mathbf{a}_k \to 0$) without changing the lattice or α. We then have a lattice with a polarizable point at each molecule, as originally proposed for acenes [1,3]. Any distribution of α on submolecules k corresponds to the $\boldsymbol{\mu}_k$ equations in (6) with all $\rho_k = 0$ and leads to a self-consistent problem for local dipolar fields. Submolecules aptly suggest a hypothetical lattice of fragments that do not overlap rather than delocalization in conjugated molecules. The opposite limit of atomic charges without induced dipoles reduces (6) to the ρ_k equation and Coulomb fields; this is the α_M limit of charges only in Tables 1 and 2. The crystal potential (5) contains both charges and dipoles. Their treatment is different, however, since ρ_k is directly accessible through the atom–atom polarizability (2) while $\boldsymbol{\mu}_k$ still comes from an assumed distribution of α_k. We expect charge flow in large conjugated molecules, and atomic charges and dipoles can readily be treated together. Their decomposition through Π into α_M and $\alpha - \alpha_M$ is convenient rather than rigorous.

Reis et al. [8] have recently discussed the linear and nonlinear responses of anthracene crystals using induced dipoles and α/TZVP-FIP (Table 1). The dielectric constant ε_{bb} is 5.25 for a single dipole at the center, 3.60 for dipoles in each ring, 3.14 for dipoles at the 14 carbons and 3.38 with an

approximation involving anisotropic Lorentz fields. Similarly large scatter are reported in the ac plane for 1, 3 and 14 submolecules, which yield $\varepsilon_{11} = 2.33$, $\varepsilon_{33} = 4.38$ and $\theta = 30.8°$. The fit with 14 carbons is satisfactory but leaves open the choice of submolecules and the omission of H atoms. These induced-dipole results are within a few percent of α/TZVP-FIP results in Table 2 for charge redistribution and the same molecular polarizability. Similar comments apply to PTCDA. The B3LYP polarizabilities in Table 1 can be attributed completely to induced dipoles at the heavy atoms by setting $\rho_k = 0 = \Pi_{kp}$ for all k, p in (6) and $\alpha_k = 0$ for H atoms. The resulting ε are $\sim$5% higher than the principal values in Table 2. Charge redistribution removes the arbitrary assignment of induced dipoles that, in sufficiently large numbers, yield comparable results for anthracene or PTCDA. Charge separation over a small distance goes smoothly into dipoles. More extended conjugation in pentacene or α-sexithiophene may sharpen the difference between charge redistribution and induced moments.

Direct evaluation of charge redistribution shifts the analysis from submolecules to comparisons of molecular and crystal data. The experimental data in Tables 1 and 2 have not been corrected for dispersion or nuclear contributions. We have not considered quadrupole moments [1] associated with π-electron density above and below the molecular plane. D_{2h} molecular symmetry is reduced to C_i in both crystals. Anthracene and PTCDA are at inversion centers and neither is strictly planar. While deviations are inconsequential (1–2%) in terms of calculated polarizabilities, they clearly point to intermolecular interactions that are neglected in oriented gases. Such quantitative issues are beyond the present work.

Acenes are alternant hydrocarbons whose atomic charges vanish rigorously in π-electron models with electron-hole symmetry and are small in higher-level theory. Induced dipoles at sp^2 centers are a natural choice. PTCDA and other molecules proposed for organic devices [25] have finite ρ_k that contribute to crystal fields. Charge redistribution governed by Π applies equally to nonalternant systems. It can also be applied as interchain interactions to NLO spectra of conjugated polymers. Responses such as third-harmonic generation, four-wave mixing, two-photon absorption and electroabsorption are modeled [26] in terms of correlated π-electronic excited states and charge redistribution in isolated strands rather than polarizable atomic orbitals.

The unit-cell polarization $\mathbf{P}(\mathbf{E})$ is the natural variable for a crystal in an applied field. The lattice polarization energy of a molecular anion, cation, or ion pair has a large electronic component that can be viewed as linear responses to internal sources. The oriented gas has Coulomb and dipolar interactions between atomic charges and induced dipoles that, in contrast to the case of submolecules, already appear in the ground state. Changes in lattice energies become the relevant variables. Energy minimization corresponds to charge redistribution in the self-consistent potential $\varphi(\mathbf{r})$ given by (8) with $\mathbf{E} = 0$. It also yields the linear (6) with fields due to fixed molecular ions. The polarization energies of fixed charges will be presented separately [12].

In summary, we have presented a new approach to electronic polarization in organic crystals. Charge redistribution is related to the atom–atom polarizability tensor Π, which gives the major part of the molecular polarizability. We obtain linear equations that generalize the self-consistent treatment of induced dipoles to include charges and compute the dielectric tensors of anthracene and PTCDA crystals.

Acknowledgements

We thank A. Kahn, S.F. Forrest and M. Hoffmann for stimulating discussions, and P. Petelenz and R.W. Munn for correspondence about induced dipoles. This work was partially supported by the National Science Foundation through the MRSEC program under DMR-9400362.

References

[1] E.A. Silinsh, V. Cápek, Organic Molecular Crystals, AIP Press, NewYork, 1994, and references therein.
[2] N.F. Mott, M.J. Littleton, Trans. Faraday Soc. 34 (1938) 485.

[3] J.W. Rohleder, R.W. Munn, Magnetism and Optics of Molecular Crystals, Wiley, New York, 1992, and references therein.
[4] D.A. Dunmur, Mol. Phys. 23 (1972) 109.
[5] P.J. Bounds, R.W. Munn, Chem. Phys. 44 (1979) 103.
[6] T. Luty, Chem. Phys. Lett. 44 (1976) 335.
[7] G. Mazur, P. Petelenz, Chem. Phys. Lett. 324 (2000) 161.
[8] H. Reis, M.G. Papadopoulos, P. Calaminici, K. Jug, A.M. Köster, Chem. Phys. 261 (2000) 359.
[9] C.A. Coulson, H.C. Longuet-Higgins, Proc. Roy. Soc. (London) A191 (1947) 39.
[10] L. Salem, The Molecular Orbital Theory of Conjugated Systems, Benjamin, New York, 1966 (Chapter 1).
[11] M.C. Zerner, G.H. Loew, R.F. Kirchner, U.T. Mueller-Westerhoff, J. Am. Chem. Soc. 102 (1980) 589.
[12] E.V. Tsiper, Z.G. Soos, Phys. Rev. B (submitted).
[13] P.P. Ewald, Ann. Phys. 64 (1921) 253.
[14] M. Born, M. Bradburn, Proc. Cambridge Philos. Soc. 39 (1943) 104.
[15] C.P. Brock, J.D. Dunitz, Acta Cryst. B 46 (1990) 795.
[16] A. Lovinger, S.R. Forrest, M.L. Kaplan, P.H. Schmidt, T. Venkatesan, J. Appl. Phys. 55 (1984) 476.
[17] A.D. Becke, J. Chem. Phys. 98 (1993) 5648.
[18] C.L. Cheng, D.S.N. Murthy, G.L.D. Ritchie, Austr. J. Chem. 25 (1972) 1301.
[19] R.J.W. LeFévre, L. Radom, G.L.D. Ritchie, J. Chem. Soc. B (1968) 775.
[20] N. Karl, H. Rohrbacher, D. Siebert, Phys. Status Solidi A 4 (1971) 105.
[21] R.W. Munn, J.R. Nicholson, H.P. Schwob, D.F. Williams, J. Chem. Phys. 58 (1973) 3828.
[22] I. Nakada, J. Phys. Soc. Jpn. 17 (1962) 113.
[23] A.N. Winchell, The Opeical Properties of Organic Compounds, second ed., Academic Press, New York, 1954.
[24] D.Y. Zang, F.F. So, S.R. Forrest, Appl. Phys. Lett. 59 (1991) 823.
[25] I.G. Hill, A. Kahn, Z.G. Soos, R.A. Pascal Jr., Chem. Phys. Lett. 327 (2000) 181.
[26] Z.G. Soos, D. Mukhopadhyay, A. Painelli, A. Girlando, in: T.A. Skotheim, R.L. Elsenbaumer, J.R. Reynolds, (Eds.), Handbook of Conducting Poymers, vol. 2, Marcel Dekker, New York, 1998, p. 165.